

## Supplementary Materials and Methods

### Subject recruitment and sampling

Healthy adult male and female volunteers (HVs) 18-40 years of age were recruited from the Washington, DC metropolitan region from September 2009 to September 2011. This natural history study was approved by the Institutional Review Board of the National Human Genome Research Institute ([clinicaltrials.gov/NCT00605878](http://clinicaltrials.gov/NCT00605878)) and all subjects provided written informed consent prior to participation. Subjects provided medical and medication history and underwent a physical examination. Exclusion criteria included history of chronic medical conditions, including chronic dermatologic diseases, and use of antimicrobials (antibiotics or antifungals) 6 months prior to sampling (see Table S1 for HV information). Bathing/showering with only non-antibacterial soap/cleansers was allowed during the 7 days prior to sample collection. No bathing, shampooing, or moisturizing was permitted for 24 hours prior to sample collection. Some HVs returned 1-3 months after their initial visit for follow-up sampling.

Fourteen skin sites representing a range of physiological characteristics and sites of predilection for fungal-associated dermatologic diseases were selected including core/proximal body sites: middle upper back, external auditory canal (inside the ear), retroauricular crease (behind the ear), occiput (back of scalp), glabella (central forehead between eyebrows), inguinal crease (skin fold midway between hip and groin area), manubrium (upper central chest), and nare (inside the nostril); and distal body sites: antecubital fossa (inner elbow), volar forearm (mid-forearm), hypothenar palm (palm of hand closer to little finger), plantar heel (bottom of heel), toenail, and toe web (webspace between 3<sup>rd</sup> and 4<sup>th</sup> toes) (Figure S1). All clinical findings observed at sampling sites were documented, including any scaling on the feet and any changes of the toenails. Body sites with left-right symmetry (10 of the 14 body sites) were sampled bilaterally to calculate intrapersonal variation (see Figure S1 for sites sampled).

### Fungal culturing and characterization

For fungal cultures, superficial skin scrapes were collected from a 4-cm<sup>2</sup> area with a sterile surgical blade and placed directly in media. Skin scrapings were spread on fungal culturing plates (under laminar flow hood to minimize contamination) to isolate pathogenic and non-pathogenic fungi, including fastidious yeasts. Selective media containing antibiotics to selectively suppress bacterial growth included: Inhibitory Mold Agar with Gentamicin; Brain Heart Infusion Agar with Chloramphenicol and Gentamicin (Remel, Lanexa, KS); and Sabouraud with Chloramphenicol and Cycloheximide (Remel, Lanexa, KS) augmented with olive oil to promote *Malassezia* growth. Plates were incubated at 30°C, checked daily for the first week and 2-3 days thereafter. Isolates that flourished in culture were re-streaked for single colonies followed by sub-culturing to ensure purity and characterized by morphological features and molecular markers. DNA was extracted with MasterPure™ Yeast DNA Purification Kit (Epicentre, Madison, WI) according to manufacturer's instruction with the addition of 5mm steel beads to mechanically disrupt fungal cell walls (Qiagen, Valencia, CA). The Internal Transcribed Spacer (ITS) 1 and 2 regions were amplified from purified genomic fungal DNA using primers 18S-F (5'-GTAAAAGTCGTAACAAGGTTTC-3') and 5.8S-1R (5'-

GTTCAAAGAYTCGATGATTCAC-3') for ITS1 and 5.8S-F (5'-GTGAATCATCGARTCTTTGAAC-3') and 28S1-R (5'-TATGCTTAAGTTCAGCGGGTA-3'). PCR products were purified and sent to ACGT, Inc. (Wheeling, IL) for sequencing and BLAST was performed on the resulting amplicon sequence to identify each isolate<sup>1</sup>.

### **Clinical sample collection, DNA extraction, PCR amplification and sequencing of 18S rRNA gene and ITS1**

For DNA analyses, samples were collected, including negative controls, as previously described<sup>2</sup>. Catch-All™ Sample Collection Swabs (Epicentre, Madison, WI) were used for skin swab sample collection across all sites with the exception of the toenail (toenail clippings were collected)<sup>3</sup>, and swabs were stored in lysis solution provided with the MasterPure™ Yeast DNA Purification Kit (Epicentre, Madison, WI). To pre-digest the toenail clippings, Proteinase K (Invitrogen, Carlsbad, CA) was added to the sample and incubated overnight with shaking at 55°C. Skin samples were incubated in yeast lysis buffer and lysozyme (20 mg/mL) for 1 hour with shaking at 37°C. Then, 5 mm steel beads were added to mechanically disrupt fungal cell walls using a TissueLyser (Qiagen, Valencia, CA) for 2 minutes at 30 Hz. The Invitrogen PureLink Genomic DNA Kit (Invitrogen, Carlsbad, CA) was utilized for all subsequent steps.

For 18S rRNA amplicon sequencing, each DNA was amplified with SR6 (5'-TACCTGGTTGATTCTGC-3') and SR1R (5'-TGTTACGACTTTTACTT-3') primers. The following PCR conditions were used: 2.5  $\mu$ l 10X AccuPrime Buffer II, 0.2  $\mu$ l Accuprime Taq, 0.5  $\mu$ l primer SR6 (20  $\mu$ M), 0.5  $\mu$ l primer SR1R (20  $\mu$ M), and 4  $\mu$ l of isolated microbial genomic DNA. PCR was performed in duplicate if possible and a portion of the reaction was run on an agarose gel to verify the presence of the 18S PCR product. Cycle number was determined such that amplification was still in the linear range of the reaction and yielded sufficient PCR product for cloning (maximum of 32 cycles). Negative controls on both the mock swab and no template DNA were performed with each set of amplifications. The PCR product was ligated into the PCR4 TOPO vector (Invitrogen, Carlsbad, CA) according to manufacturer's protocol. 384 resulting bacterial colonies per ligation were picked, plasmid DNA purified and inserts sequenced at NISC on an ABI 3730xl sequencer (Applied Biosystems Inc., Foster City, CA) using M13 primers flanking the insert.

For ITS1 amplicon sequencing, each DNA was amplified with adapter+18SF (5'-CCTATCCCCTGTGTGCCTTGGCAGTCTCAGGTAAGTCGTAACAAGGTTTC) and 5.8S-1R+ barcode (5'-GTTCAAAGAYTCGATGATTCAC) primers<sup>4</sup>. The following PCR conditions were used: 2.5  $\mu$ l 10X AccuPrime Buffer II, 0.2  $\mu$ l Accuprime Taq (Invitrogen, Carlsbad, CA), 0.1  $\mu$ l primer B adapter+18SF (100  $\mu$ M), 2  $\mu$ l primer 5.8S-1R+barcode (5  $\mu$ M), and 4  $\mu$ l of isolated microbial genomic DNA. The PCR was performed in duplicate for 32 cycles. Duplicate amplicons were combined, purified (Agencourt AMPure XP-PCR Purification Kit (Beckman Coulter, Inc., Brea, CA)), and quantified (QuantIT dsDNA High-Sensitivity Assay Kit (Invitrogen, Carlsbad, CA)). An average of ~8 ng DNA of 94 amplicons were pooled together, purified (MinElute PCR Purification Kit (Qiagen, Valencia, CA)) and sequenced on a Roche 454 GS20/FLX platform with Titanium chemistry (Roche, Branford, Connecticut). Flow-grams were processed with the 454 Basecalling pipeline (v2.5.3).

For 16S, amplicon sequencing, each DNA was amplified with adapter+V1\_27F (5'-CCTATCCCCTGTGTGCCTTGGCAGTCTCAGAGAGTTTGATCCTGGCTCAG) and V3\_534R+barcode primers (5'- CAGCACGCATTACCGCGGCTGCTGG)<sup>4</sup>. The following PCR conditions were used: 2  $\mu$ l 10X AccuPrime Buffer II, 0.15  $\mu$ l Accuprime Taq (Invitrogen, Carlsbad, CA), 0.04  $\mu$ l adapter+V1\_27F (100  $\mu$  M), 2  $\mu$ l primer V3\_354R+barcode (2  $\mu$  M), and 2  $\mu$ l of isolated microbial genomic DNA. PCR was performed in duplicate for 30 cycles and then PCR-clean up, amplicon pooling of ~10 ng DNA, purification, and sequencing were performed as described above for ITS.

### **Custom generated fungal ITS1 reference database**

ITS sequences were extracted from GenBank using the query: (ITS1[All Fields] OR ITS2[All Fields] OR 5.8S[All Fields]) AND Fungi[All Fields] NOT "uncultured"[All Fields]. Taxonomy classifications associated with sequences were recorded as strings in the following order: kingdom, phylum, class, order, family and genus, and recorded as unclassified if the levels were not clearly defined. Sequence classification was manually curated and any discrepancies in taxonomy strings were resolved using the Taxonomy database in Pubmed. When both anamorphic (asexual) and teleomorphic (sexual) names were represented for a species within GenBank, the strings were manually curated and the anamorphic taxonomic nomenclature was selected. The sequences were then clustered to 95% sequence identity using CD-HIT<sup>5</sup>. Representative sequences were chosen by CD-HIT and a consensus taxonomy string was generated for the sequence, starting from the highest level (kingdom) and moving to the lowest level (genus). If the most highly represented classification was twice as frequent as the next one, this classification was chosen for the level. If no classification satisfied this criterion, this and all lower levels were set as unclassified. Sequences clearly misclassified as fungi were removed from the curated database.

### **Sequence classification and analyses**

Sequences were pre-processed to remove primers and barcodes. Possible chimeras created during PCR amplification were identified with UCHIME in mothur<sup>6,7</sup>. Reference was set to self and included in the names file to check for chimeras using more abundant sequences as references<sup>7</sup>. With the ITS database described above as the reference, these chimera checked sequences were classified to the genus level with the BLAST option and the k-Nearest Neighbor (knn) algorithm in mothur<sup>7</sup>. 16S rRNA sequences were classified to the genus or species level using the RDP classifier with training set (v6) and as previously described<sup>8</sup>. Sequences were assigned to taxonomic units based on their genus level phylogenetic classification. R statistical software was implemented to generate plots representing the relative abundance of fungal genera.

Community richness (Chao1), diversity (Shannon Index), membership (Jaccard Index) and structure (Theta Index) were calculated within mothur as previously described after using a subsampling cutoff of 1000 sequences/sample<sup>2,9,10</sup>. Diversity indices for left and right symmetric sites were averaged for body sites with bilateral symmetry. All statistical analyses are represented as the standard error of the mean (SE) unless otherwise indicated.

### **18S rRNA sequence classification**

To pre-process the 18S rRNA sequences, traces were base called using Phred (v 0.990722.g), trimmed with Crossmatch, and each clone assembled using Phrap (v 0.990329). The default parameters were used except force level was 9 and the mismatch penalty was -1<sup>11,12</sup>. For approximately 15% of read pairs, the overlap was not sufficient for de novo assembly and a scaffolded assembly was attempted. Scaffolded assembly was done using the AmosCmp16Spipeline (available from <http://microbiomeutil.sourceforge.net>) and non-redundant reference sequences from the SILVA small subunit rRNA database<sup>13</sup>. 18S rRNA sequences were classified using the SILVA v108 database. R was implemented to generate plots representing the relative abundance of fungal genera.

### **Malassezia sequence classification to the species level**

To classify *Malassezia* ITS1 sequences from the genus to species level, we used the `get.lineage` command in `mothur` to retrieve only *Malassezia* sequences. As an internal check, these skin-associated *Malassezia* ITS1 sequences were aligned with the *Malassezia* reference package in `mothur`, and all discrepancies resolved. Next, we curated and aligned a reference library of *Malassezia* type-strain ITS1 sequences retrieved from GenBank augmented by those from the fungal cultures described above. Two to ten representatives were included in the database for *Malassezia* species (*M. globosa*, *M. restricta*, *M. sympodialis*, *M. slooffiae*, *M. furfur*, *M. pachydermatis*, *M. dermatis*, *M. yamatoensis*, *M. obtusa*, *M. japonica*, and *M. nana*) for a total of 52 ITS1 sequences. Sequences were aligned with MUSCLE to generate the reference alignment<sup>14</sup>.

This curated library was used as the reference to phylogenetically place and classify novel skin-associated *Malassezia* ITS1 sequences to the species level with the software package *pplacer*<sup>15</sup>. Sequence placement on the reference tree along with confidence scores were visualized in Archaeopteryx using the *guppy* command<sup>15,16</sup>. *guppy* classify and a light-weight SQL database were employed to make and store taxonomic classifications. A likelihood score of at least 0.65 was used for classifications produced by the *guppy* classify command. Finally, classifications were converted into `mothur` compatible taxonomic strings to create the `tax.summary` file for community-based analyses as above. Similarly, species-level designations for bacterial *Staphylococcus* sequences were generated using *pplacer* with a 16S rRNA reference database built from rRNA records extracted from RefSeq genomes (as of April 2012) and RDP type species sequences (Release 10, Update 24)<sup>8</sup>.

### **ITS1 and 16S comparisons**

Taxonomic units were defined from genus- and, where available, species-level ITS and 16S rRNA phylotypes. Groups were each subsampled to 1800 sequences and the Yue-Clayton theta index generated to compare the similarity between communities. Principal coordinate analysis of the theta index was performed and the Spearman correlation of the relative abundance of each taxonomic unit versus the top three axes was calculated to assess how each taxonomic unit contributed to variation along the axes.

Co-occurrence between bacteria and fungi was assessed by calculating the partial Spearman correlation of the relative abundances of the different taxa, adjusted for multiple within-patient measurements. Calculations were performed on Fisher-transformed *r* values. Comparisons were limited to those taxa which occurred in >25% of

samples for either ITS or 16S rRNA, and for ITS, if mean abundance across all samples exceeded 0.25%. Because of the relatively higher fungal diversity, only feet sites (Ph, Tn, and Tw) were used.

## References

1. Altschul, S.F., Gish, W., Miller, W., Myers, E.W. & Lipman, D.J. Basic local alignment search tool. *J Mol Biol* **215**, 403-10 (1990).
2. Grice, E.A. *et al.* Topographical and temporal diversity of the human skin microbiome. *Science* **324**, 1190-2 (2009).
3. Grice, E.A. *et al.* A diversity profile of the human skin microbiota. *Genome Res* **18**, 1043-50 (2008).
4. Lennon, N.J. *et al.* A scalable, fully automated process for construction of sequence-ready barcoded libraries for 454. *Genome Biol* **11**, R15 (2010).
5. Li, W. & Godzik, A. Cd-hit: a fast program for clustering and comparing large sets of protein or nucleotide sequences. *Bioinformatics* **22**, 1658-9 (2006).
6. Edgar, R.C., Haas, B.J., Clemente, J.C., Quince, C. & Knight, R. UCHIME improves sensitivity and speed of chimera detection. *Bioinformatics* **27**, 2194-200 (2011).
7. Schloss, P.D. *et al.* Introducing mothur: open-source, platform-independent, community-supported software for describing and comparing microbial communities. *Appl Environ Microbiol* **75**, 7537-41 (2009).
8. Conlan, S., Kong, H.H. & Segre, J.A. Species-level analysis of DNA sequence data from the NIH Human Microbiome Project. *PloS one* **7**, e47075 (2012).
9. Kong, H.H. *et al.* Temporal shifts in the skin microbiome associated with disease flares and treatment in children with atopic dermatitis. *Genome Res* **22**, 850-9 (2012).
10. Yue, J.C. & Clayton, M.K. A similarity measure based on species proportions. *Communications in Statistics-Theory and Methods* **34**, 2123-2131 (2005).
11. Ewing, B. & Green, P. Base-calling of automated sequencer traces using phred. II. Error probabilities. *Genome Res* **8**, 186-94 (1998).
12. Ewing, B., Hillier, L., Wendl, M.C. & Green, P. Base-calling of automated sequencer traces using phred. I. Accuracy assessment. *Genome Res* **8**, 175-85 (1998).
13. Pruesse, E. *et al.* SILVA: a comprehensive online resource for quality checked and aligned ribosomal RNA sequence data compatible with ARB. *Nucleic Acids Res* **35**, 7188-96 (2007).
14. Edgar, R.C. MUSCLE: multiple sequence alignment with high accuracy and high throughput. *Nucleic Acids Res* **32**, 1792-7 (2004).
15. Matsen, F.A., Kodner, R.B. & Armbrust, E.V. pplacer: linear time maximum-likelihood and Bayesian phylogenetic placement of sequences onto a fixed reference tree. *BMC Bioinformatics* **11**, 538 (2010).
16. Han, M.V. & Zmasek, C.M. phyloXML: XML for evolutionary biology and comparative genomics. *BMC Bioinformatics* **10**, 356 (2009).

## **SUPPLEMENTAL FIGURES AND TABLES**

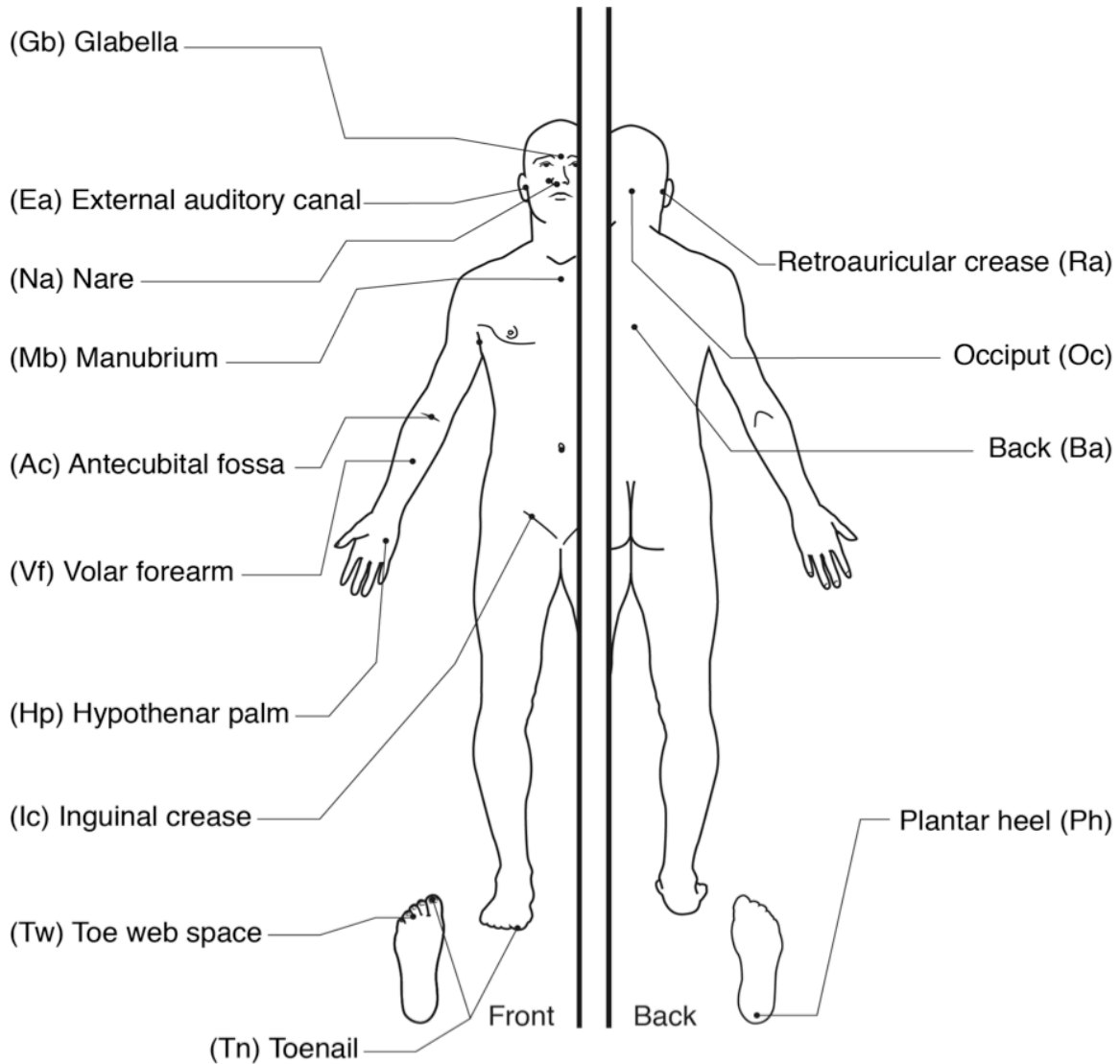


**Figure S1. Body sites sampled in healthy adult volunteers.**

Location of 14 body sites selected for the fungal diversity survey. Two letter codes for body sites are indicated in parentheses.

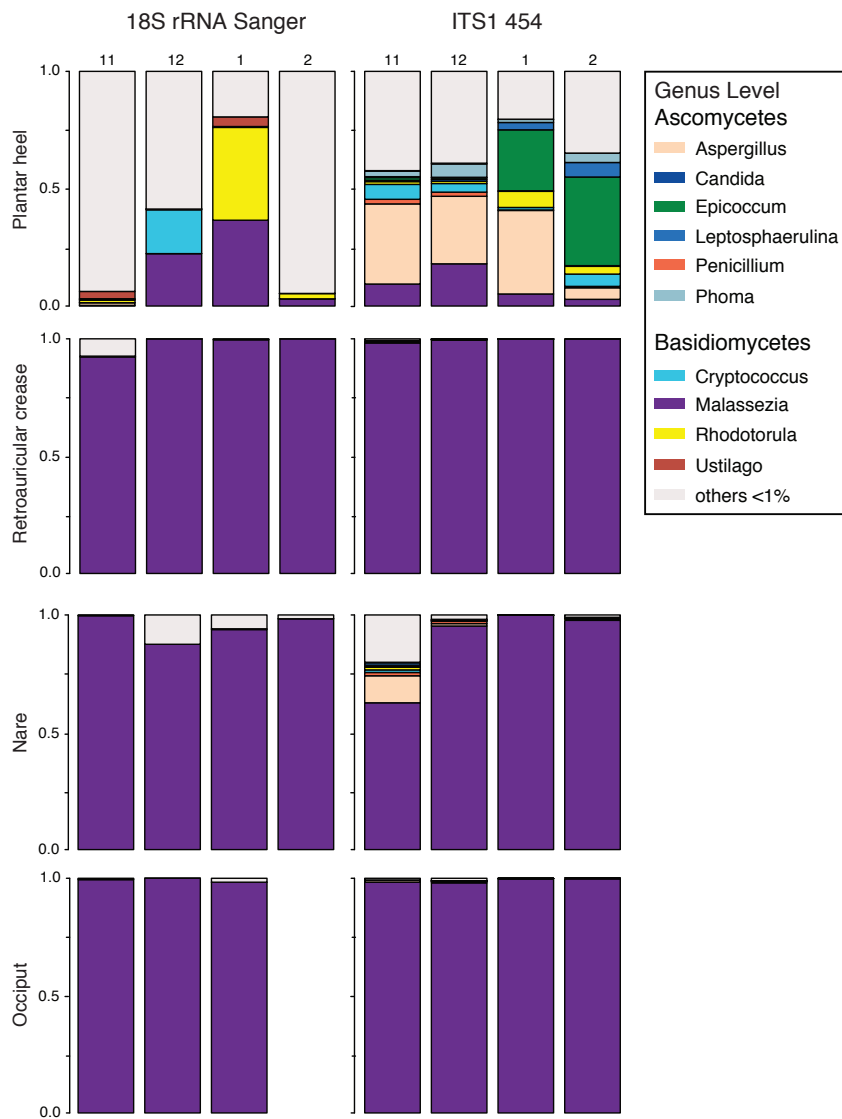


**Figure S2. Fungal 18S rRNA and ITS skin survey.**

Fungal 18S rRNA was sequenced with Sanger chemistry in four HVs across 4 body sites. ITS1 was sequenced on 454/Roche instrument in the same subset of HVs. Fungal sequences were taxonomically classified to the genus level relative to Silva and custom database for 18S rRNA and ITS sequences, respectively. HV# provided at top.



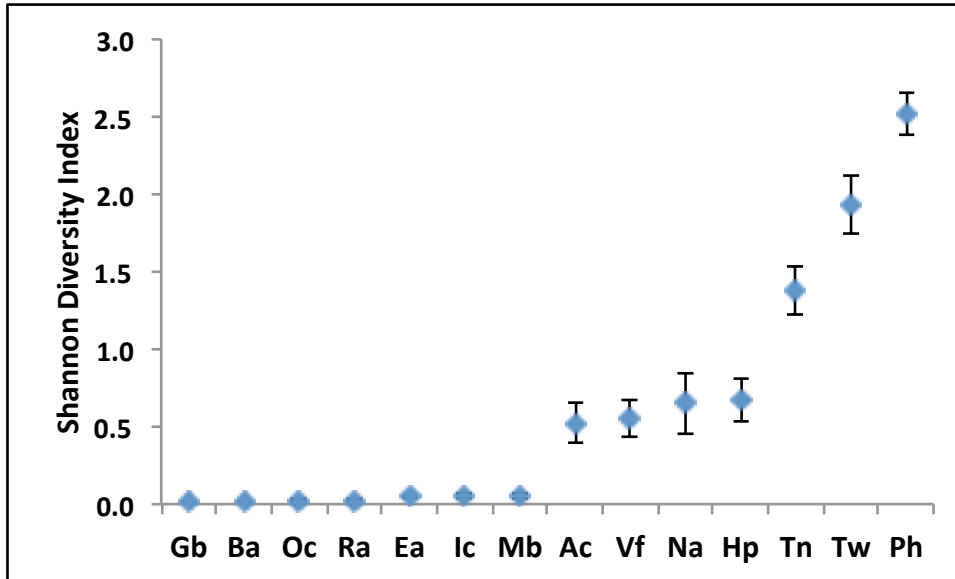


**Figure S3. Mean Shannon Diversity of body sites.**

Mean fungal diversity of body sites measured with the Shannon Diversity Index. Error bars represent the standard error of the mean. Fungal samples from initial and return visits are combined by body site. The outlier, HV7, was excluded from this analysis. Two letter codes for body sites are defined in Figure S1.

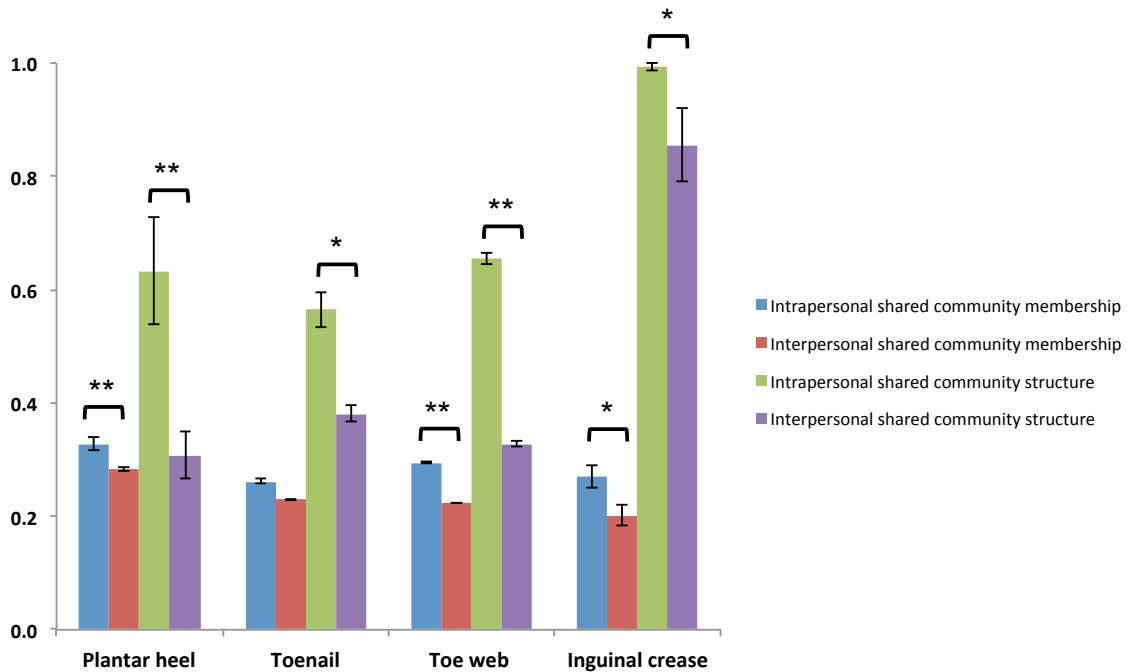


**Figure S4. Intrapersonal vs. Interpersonal variation at four body sites prone to fungal infection.**

Intrapersonal and interpersonal variations were determined by Jaccard (community membership) and Theta (community structure). Intrapersonal variation is calculated by comparing left and right symmetric sites on the same individual. Interpersonal variation is calculated by comparing an individual to others surveyed at the same body site. Four body sites are shown: plantar heel, toenail, toe web, and inguinal crease. Error bars represent the standard error of the mean. We performed pair-wise calculations for all HVs at each site using the one-tailed paired *t* test. The *P* values for the Jaccard and Theta indices are \*= $p < 0.05$ ; \*\*= $p < 0.01$ .

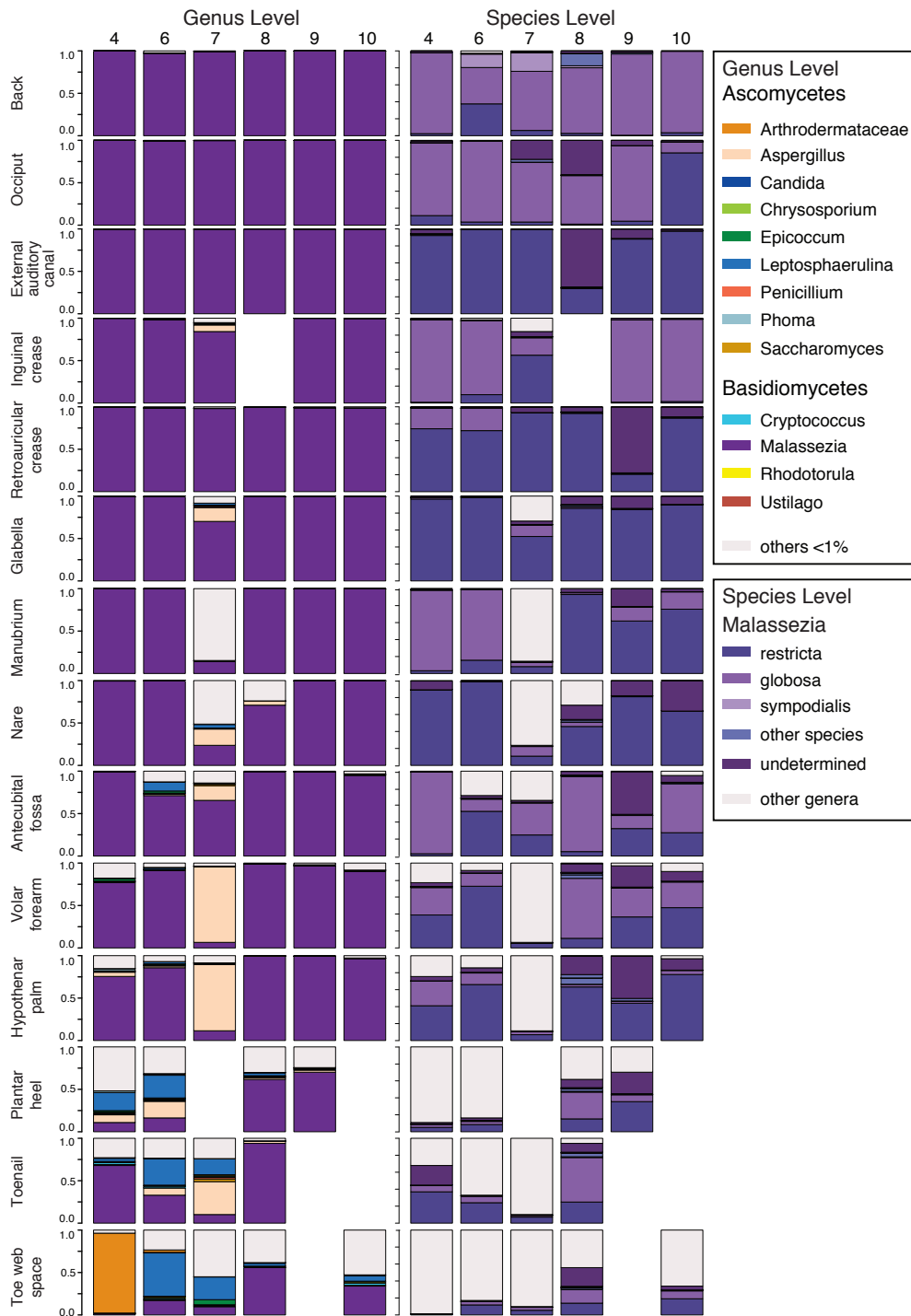


**Figure S5. Relative abundance of fungal genera and *Malassezia* species of healthy volunteers resampled 1-3 months later.**

Individual body sites across 6 HVs resampled 1-3 months after initial visit were taxonomically classified to the genus level using a custom-generated ITS fungal reference database. *Malassezia* species were resolved to the species level with custom curation and the program *pplacer*. HV# provided at top.

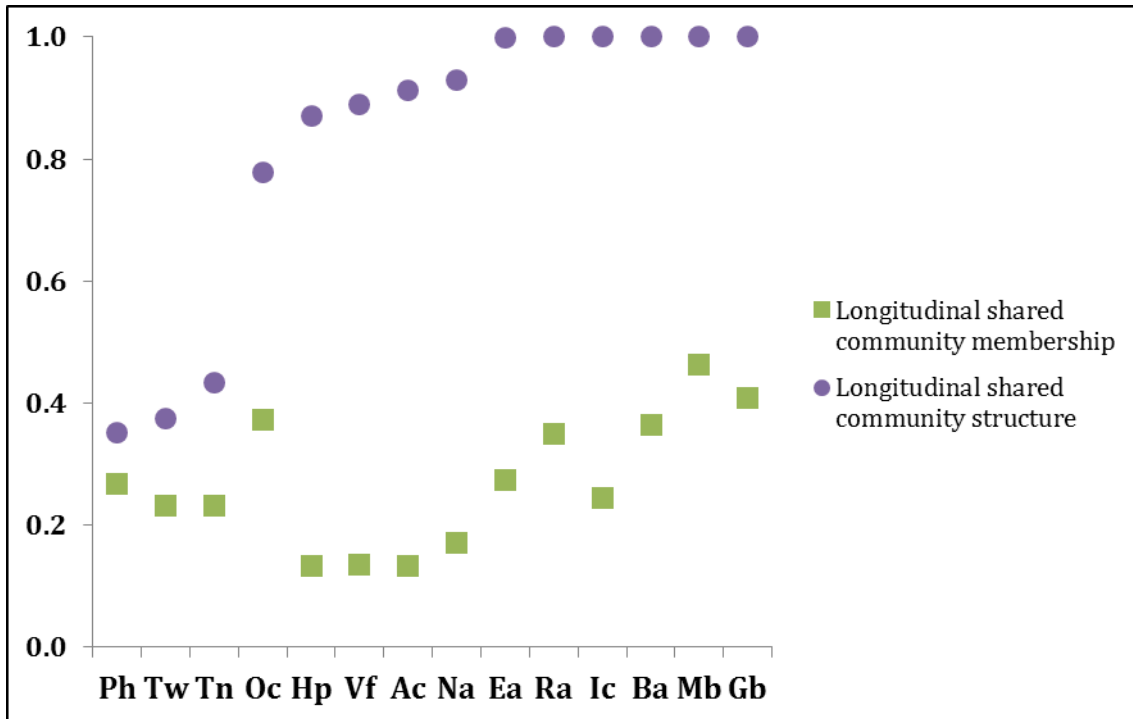


**Figure S6. Longitudinal stability is site dependent.**

Longitudinal stability of fungal microbial community membership and structure over time are calculated as Jaccard and Theta, respectively, within mothur. This analysis compares initial and return sampling for five HVs. HV7 was excluded as an outlier from the final analysis. Jaccard and Theta values range from 0 to 1 with larger values representing greater stability. Two letter codes for body sites are defined in Figure S1.

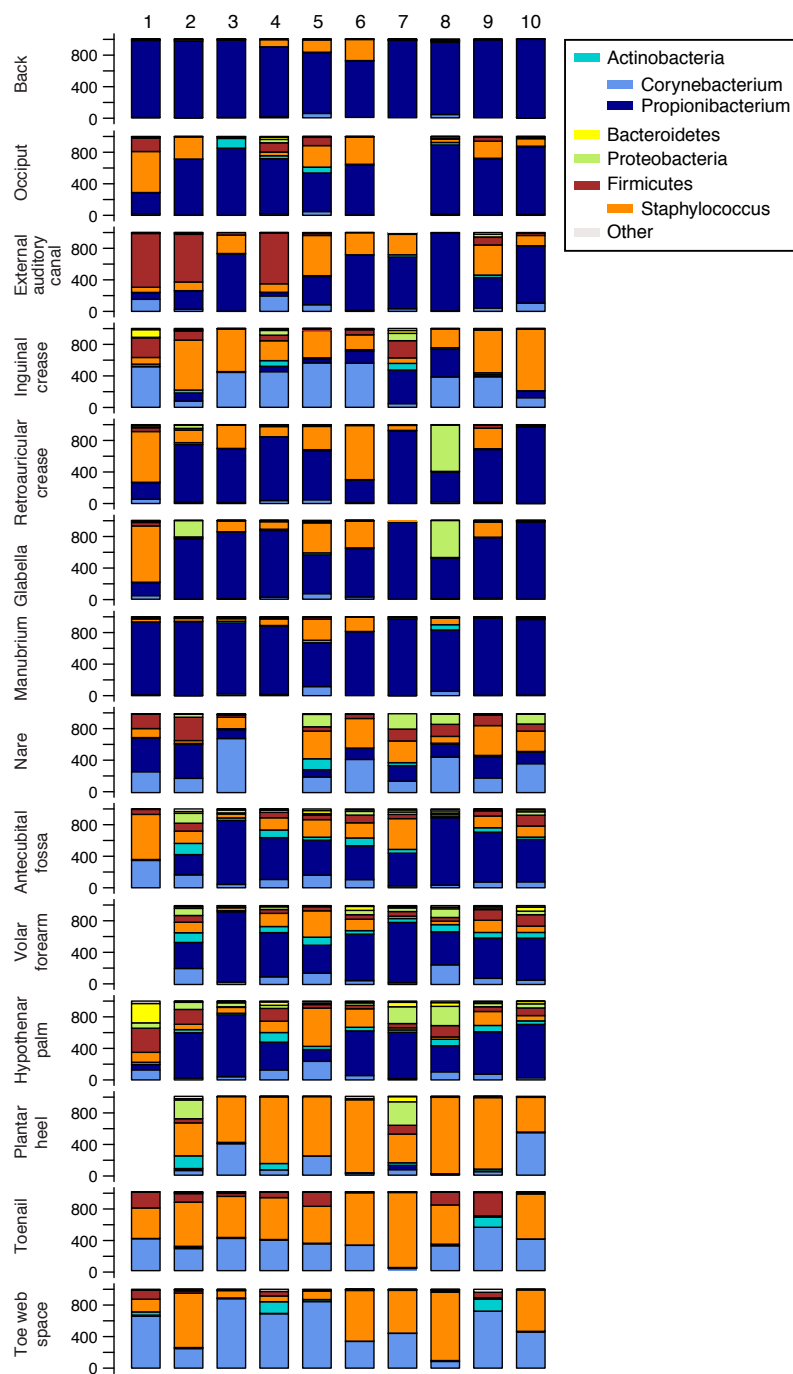


**Figure S7. Bacterial relative abundance.**

Individual body sites across all 10 HVs were taxonomically classified to the genus level using the RDP classifier and training set (v6). Data from the left side is displayed for symmetrical sites.

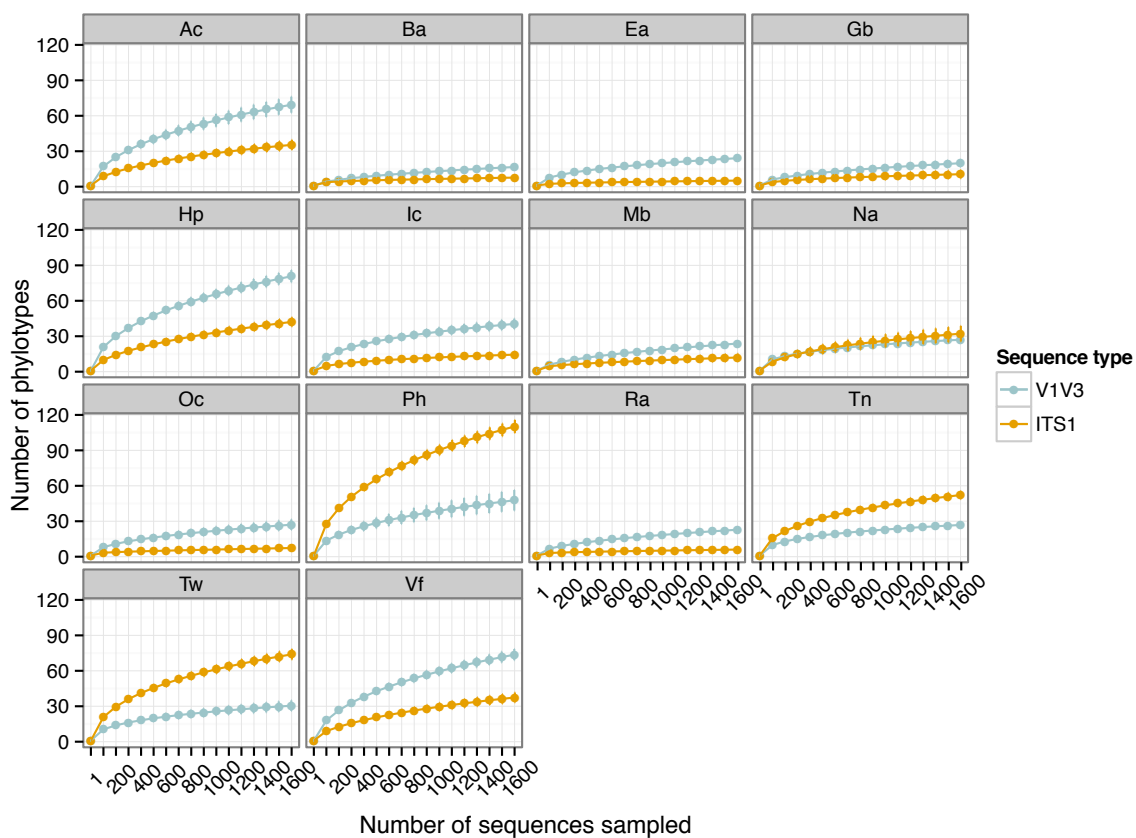


**Figure S8. Richness accumulation diverges between fungal and bacterial communities in a site-dependent manner.** Rarefaction analysis for fungal and bacterial communities using genus, and where available, species-level phylotypes. Two letter codes for body sites are defined in Figure S1. Each point represents mean  $\pm$  SEM of all individuals at specified site for either fungi (orange) or bacteria (blue).

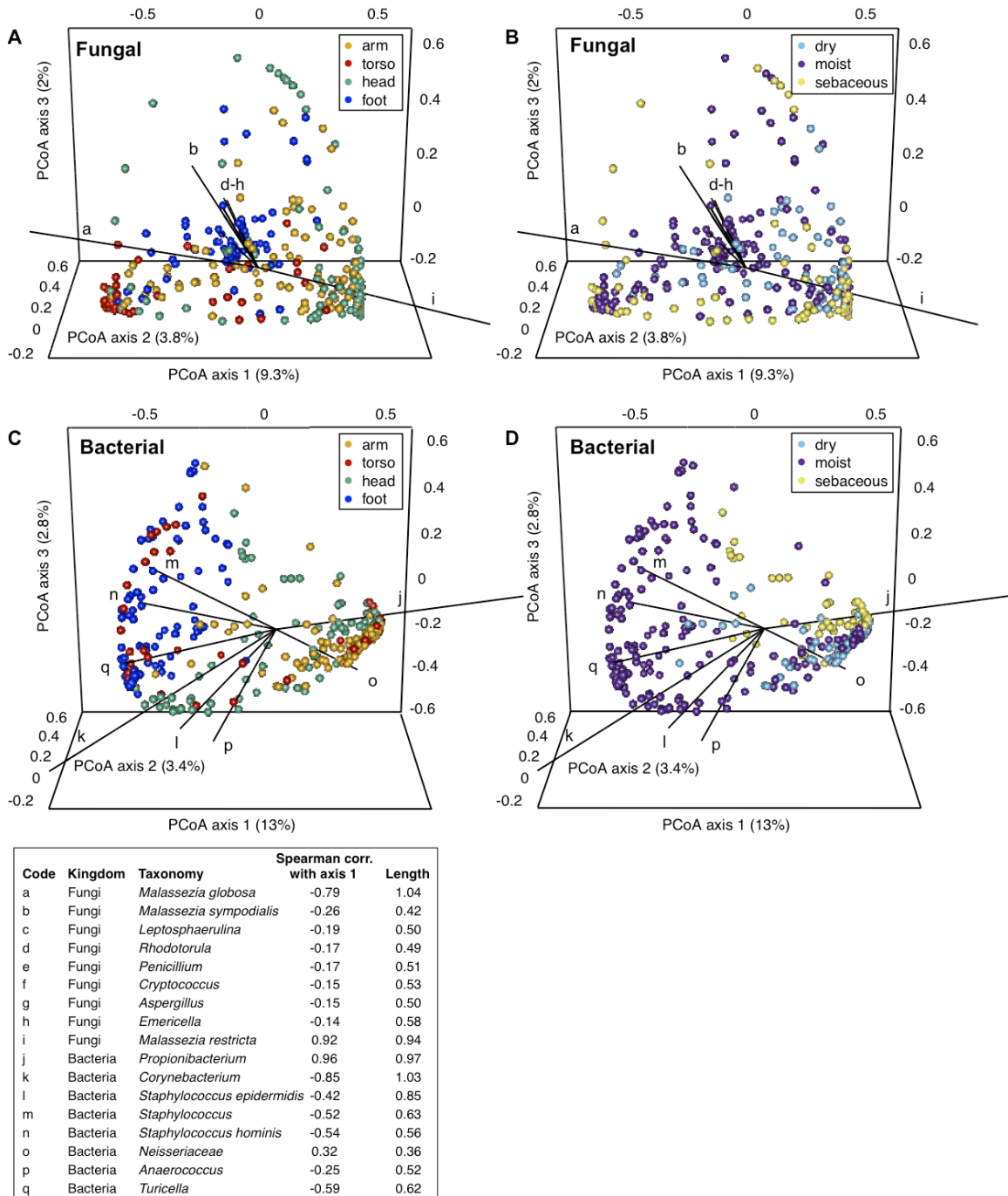


**Figure S9. Forces shaping fungal and bacterial communities.** Principal coordinates analysis (PCoA) of degree of similarity of fungal and bacterial communities, based on predominant genera and species. Variation in fungal communities clustered by site location (A) compared with site physiology (B). Bacterial community structure was more dependent on site physiology (C) than site location (D). Axes that most significantly contribute to variation and their relative length are defined in the legend.

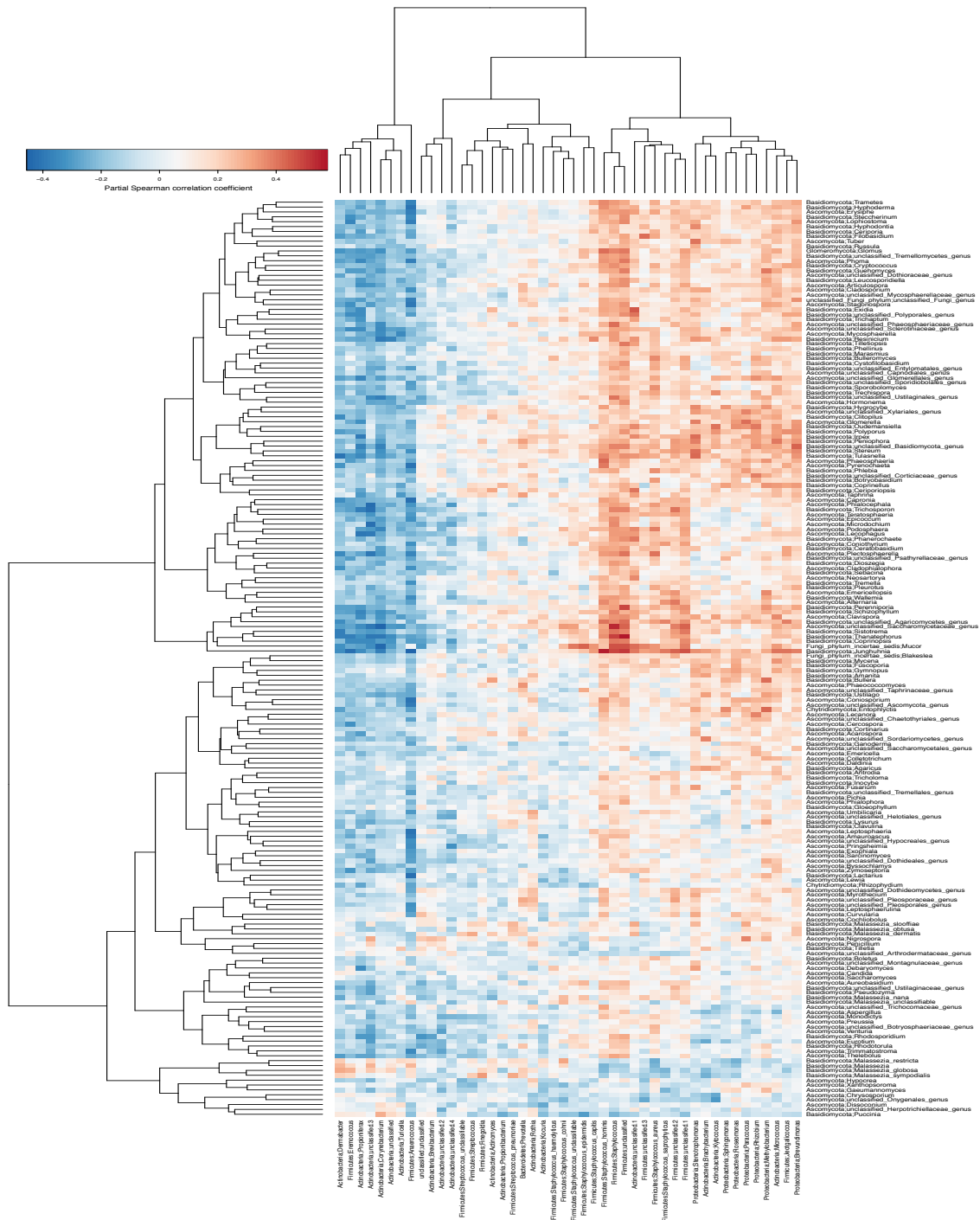


**Figure S10. Correlations of relative abundances of fungal and bacterial phylotypes in the feet.** Correlations were analyzed for fungal and bacterial genera, and when possible species, that occurred in >25% of plantar heel, toenail, or toeweb samples. Partial Spearman correlations between relative abundances of fungal vs. bacterial phylotypes were calculated, adjusting for multiple subject measurements. Two-way unsupervised hierarchical clustering of the Spearman correlation coefficients was then performed. Reds indicate correlation; blues indicate anti-correlation.



Sample ID	Sex	Clinically involved		
		Tw	Tn	Ph
HV1	Male	-	-	-
HV2	Female	-	-	-
HV3	Female	-	L <sup>o</sup>	R <sup>o</sup> /L
HV4*	Male	-	-	-
HV5	Male	-	-	-
HV6*	Male	R/L	-	-
HV7*	Female	-	R <sup>o</sup> /L	-
HV8*	Male	-	-	-
HV9*	Male	R/L	-	-
HV10*	Female	R	-	R/L
HV11**	Male	-	-	-
HV12**	Male	-	-	-

**Table S1. Clinical summary of healthy adult volunteer data.**

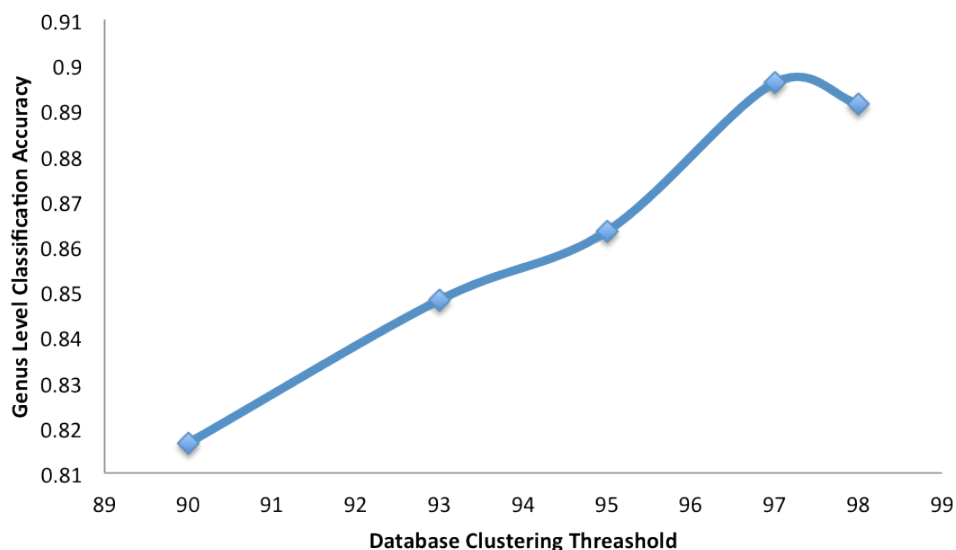
Brief summary of the study participants: sample IDs, sex, and foot sites, which were clinically involved during initial visits. Clinically involved was defined as scaling or toenail changes present at sampling site. \* indicates the 6 of 10 healthy volunteers re-sampled approximately 1-3 months after initial sampling. \*\* indicates additional two healthy volunteers for 18S versus ITS comparison (see Fig S2). <sup>o</sup> indicates the samples which had positive mycological cultures. Two letter codes for specific body sites are defined in Figure S1. R denotes right side; L denotes left side.

<b>Genera</b>	<b>Number of isolates cultured across skin sites in all HVs</b>
<i>Alternaria</i>	1
<i>Aspergillus</i>	19
<i>Candida</i>	1
<i>Chaetomium</i>	1
<i>Chrysosporium</i>	3
<i>Cladosporium</i>	4
<i>Coprinellus</i>	2
<i>Malassezia</i>	62
<i>Mucor</i>	1
<i>Nigrospora</i>	1
<i>Penicillium</i>	25
<i>Pestalotiopsis</i>	2
<i>Rhodotorula</i>	5
<i>Saccharomyces</i>	1
<i>Sclerostagonospora</i>	1
<i>Scolecobasidium</i>	1
<i>Thielavia</i>	1
<i>Trichophyton</i>	4

**Table S2. List of cultured genera from culture-based approach.**

Genera isolated from the initial sampling of skin sites are listed with number of individual isolates cultured.

## Database Accuracy



%id clustering	seconds for classification (1000 sequences)	genus level accuracy	overall accuracy
90	94	0.8165888	0.9584059
93	118	0.8481308	0.965177
95	150	0.8633178	0.9669182
97	198	0.896028	0.9746566
98	242	0.8913551	0.9729155

**Table S3. Fungal ITS database accuracy.**

To test the accuracy of the custom generated fungal database, ITS1 sequences were identified in GenBank, perturbed (trimmed to smaller sub-fragments or bases altered) and then re-classified using the custom database at different clustering thresholds. Accuracy peaks at the 97% identity cutoff. However, we chose a more conservative 95% identity-clustering cutoff to avoid the possibility of over fitting to the data.

	Initial Sampling										Re-sampling					
	HV1	HV2	HV3	HV4	HV5	HV6	HV7	HV8	HV9	HV10	HV4-2	HV6-2	HV7-2	HV8-2	HV9-2	HV10-2
<b>AcLSw</b>	11165	7265	12788	22858	28698	9208	6164	12400	20898	26541	26615	13191	23927	10537	7342	5513
<b>AcRSw</b>	9127	7704	9092	23026	40239	7197	7265	28067	11976	8293	17058	8109	19879	8589	6064	9230
<b>BaCSw</b>	9506	13142	4680	26967	16210	16967	8518	65859	15959	41979	17388	2772	14338	8148	9190	9761
<b>EaLSw</b>	10881	11144	11529	15626	8317	23831	19066	56149	8703	12106	14995	17500	12695	15078	3462	8128
<b>EaRSw</b>	18923	12561	8951	13979	12048	11326	6039	88102	9516	13542	14934	23560	10210	12894	6613	5647
<b>GbCSw</b>	9351	15220	9346	47687	15844	23840	8297	36232	21615	12820	13659	15472	12885	25749	7201	5119
<b>HpLSw</b>	9459	7341	11493	14036	202082	7423	7583	26323	11116	17589	12538	7621	11413	6191	8394	11125
<b>HpRSw</b>	7963	22932	8035	10037	15912	9316	6200	21194	15275	15585	8448	5486	12212	8839	22034	7186
<b>IcLSw</b>	29300	10025	8181	27259	16095	20327	5289	57312	11583	6625	15864	20624	35345	111	12066	3317
<b>IcRSw</b>	12322	11342	4478	28534	18060	16966	5898	35192	25672	8346	11614	12952	5385	44857	6292	9263
<b>NbCSw</b>	9153	20980	5751	38914	18811	17180	8169	29188	6417	17213	16014	10315	12485	11910	7059	6759
<b>NaLSw</b>	12386	12727	12200	6681	4392	19590	6563	14796	28120	26341	26008	18506	15368	7458	5826	8261
<b>NaRSw</b>	17453	8905	7363	6080	6774	12143	6073	21403	19528	26309	16555	18466	8459	5536	9456	4564
<b>OcCSw</b>	8140	13497	10228	28799	25182	19722	12910	25945	20377	54560	11207	37349	19877	21093	9420	8675
<b>PhLSw</b>	55173	9422	6047	11191	16679	15577	60474	14532	13788	9879	17151	2767	LRC	3573	5823	LRC
<b>PhRSw</b>	21046	5737	LRC	9820	22812	11643	5892	5986	7184	13404	14191	5957	2597	5688	4048	LRC
<b>RaLSw</b>	10884	12158	8843	22849	29343	15982	16397	18738	16371	19156	9835	13791	12904	14828	6530	6474
<b>RaRSw</b>	10524	12727	11801	22305	21252	13791	17354	14185	25670	10242	12659	19841	30194	13195	5119	6660
<b>TnLCut</b>	5031	16039	12172	9203	8786	14938	127	23828	17068	106381	2881	8622	7361	5396	LRC	LRC
<b>TnRCut</b>	4326	8569	22197	4450	17447	6692	9747	16889	10175	9139	3431	8825	9242	4025	5094	4163
<b>TwLSw</b>	11008	43413	3539	12254	12407	6598	9291	34340	50687	8773	15041	5437	15607	1989	LRC	3921
<b>TwRSw</b>	7417	12461	9735	24951	16670	8669	10471	4503	16856	8570	8897	9041	6805	3302	2574	3824
<b>VfLSw</b>	9289	21453	5096	24877	14644	12989	6824	18186	26960	14989	2778	29491	18828	7229	6486	7071
<b>VfRSw</b>	8063	27726	7061	11541	24401	11799	6883	27701	55602	18305	50089	62573	13365	5364	2356	4933

**Table S4. Total number of fungal ITS1 sequences at each body site.**

Number of sequences generated and analyzed for each body site in the 10 initial HVs (indicated by HV#) and the 6 resampled HVs (indicated by HV#-2). The resampled HVs were sampled ~1-3 months after the initial sampling. LRC denotes samples with a Low Read Count, <100 sequences. Codes for samples are two letter codes for body sites as defined in Figure S1; L=left, R=right and C=center; Sw=swab and Cut=cut (for toenail).

<b>Shannon</b>	<b>Initial Mean</b>	<b>Initial Standard Error</b>	<b>Return* Mean</b>	<b>Return* Standard Error</b>
<b>Gb</b>	<b>0.01</b>	<b>0.01</b>	<b>0.003</b>	<b>0.002</b>
<b>Ba</b>	<b>0.02</b>	<b>0.01</b>	<b>0.039</b>	<b>0.035</b>
<b>Oc</b>	<b>0.02</b>	<b>0.01</b>	<b>0.461</b>	<b>0.099</b>
<b>Ra</b>	<b>0.02</b>	<b>0.01</b>	<b>0.013</b>	<b>0.003</b>
<b>Ea</b>	<b>0.05</b>	<b>0.01</b>	<b>0.047</b>	<b>0.027</b>
<b>Ic</b>	<b>0.06</b>	<b>0.02</b>	<b>0.044</b>	<b>0.015</b>
<b>Mb</b>	<b>0.06</b>	<b>0.02</b>	<b>0.005</b>	<b>0.002</b>
<b>Ac</b>	<b>0.52</b>	<b>0.13</b>	<b>0.359</b>	<b>0.152</b>
<b>Vf</b>	<b>0.55</b>	<b>0.12</b>	<b>0.512</b>	<b>0.164</b>
<b>Na</b>	<b>0.65</b>	<b>0.19</b>	<b>0.258</b>	<b>0.163</b>
<b>Hp</b>	<b>0.67</b>	<b>0.14</b>	<b>0.639</b>	<b>0.241</b>
<b>Tn</b>	<b>1.38</b>	<b>0.16</b>	<b>1.515</b>	<b>0.336</b>
<b>Tw</b>	<b>1.93</b>	<b>0.19</b>	<b>2.222</b>	<b>0.251</b>
<b>Ph</b>	<b>2.52</b>	<b>0.13</b>	<b>2.237</b>	<b>0.282</b>

**\*Data available only for 6/10 resampled HVs**

**Table S5. Mean Shannon Diversity values.**

Shannon Diversity values were calculated within mothur at the genus level. Table denotes initial visits and \* indicates values for the resampled HVs. SE represents the standard error of the mean. Two letter codes for body sites are defined in Figure S1.

	16S Median	16S Median Absolute Deviation	ITS Median	ITS Median Absolute Deviation
Ac-L	54	12.5	18	13.5
Ba-C	11	4.5	2.5	1.5
Ea-L	12.5	5.5	2	1
Gb-C	13	3.5	2	1
Hp-L	66.5	9.5	29.5	7.5
Ic-L	24	13.5	4.5	1.5
Mb-C	20	3.5	5.5	2.5
Na-L	21	5	9.5	7
Oc-C	16	6.5	2.5	1.5
Ph-L	17	6.5	79.5	17.5
Ra-L	13	2.5	2	1
Tn-L	17	4	41	9.5
Tw-L	16.5	2.5	59.5	15.5
Vf-L	58	22.5	24	10.5

**Table S6. Richness correlation of 16S and ITS.**

Chao1 richness values were calculated within mothur at the phylogenetic level of genera for the initial visit sampling of only the left body sites. This table displays the median richness and median absolute deviation for bacteria (16S) and fungi (ITS). Two letter codes for body sites are defined in Figure S1. L=left; C = center.

<b>Body site</b>	<b>HV</b>	<b>Jaccard Intra</b>	<b>Jaccard Inter</b>	<b>Theta Intra</b>	<b>Theta Inter</b>
<b>Plantar heel</b>	<b>1</b>	<b>0.3306</b>	<b>0.2697</b>	<b>0.0724</b>	<b>0.1597</b>
	<b>2</b>	<b>0.3684</b>	<b>0.2748</b>	<b>0.6553</b>	<b>0.1626</b>
	<b>4</b>	<b>0.2857</b>	<b>0.2752</b>	<b>0.8226</b>	<b>0.4278</b>
	<b>5</b>	<b>0.3282</b>	<b>0.2975</b>	<b>0.9513</b>	<b>0.4229</b>
	<b>6</b>	<b>0.3107</b>	<b>0.2823</b>	<b>0.8177</b>	<b>0.1308</b>
	<b>7</b>	<b>0.3067</b>	<b>0.2926</b>	<b>0.4506</b>	<b>0.3209</b>
	<b>8</b>	<b>0.3007</b>	<b>0.2920</b>	<b>0.6738</b>	<b>0.3482</b>
	<b>9</b>	<b>0.3302</b>	<b>0.2840</b>	<b>0.3832</b>	<b>0.3745</b>
	<b>10</b>	<b>0.3876</b>	<b>0.2760</b>	<b>0.8694</b>	<b>0.4214</b>
	<b>Toenail</b>	<b>1</b>	<b>0.2456</b>	<b>0.2356</b>	<b>0.6855</b>
<b>2</b>		<b>0.2836</b>	<b>0.2577</b>	<b>0.1051</b>	<b>0.0745</b>
<b>3</b>		<b>0.0833</b>	<b>0.1437</b>	<b>0.0084</b>	<b>0.3009</b>
<b>4</b>		<b>0.1370</b>	<b>0.1961</b>	<b>0.8492</b>	<b>0.5228</b>
<b>5</b>		<b>0.2973</b>	<b>0.2484</b>	<b>0.9363</b>	<b>0.5382</b>
<b>6</b>		<b>0.3896</b>	<b>0.2578</b>	<b>0.8072</b>	<b>0.2564</b>
<b>8</b>		<b>0.2679</b>	<b>0.2336</b>	<b>0.9951</b>	<b>0.5421</b>
<b>9</b>		<b>0.2933</b>	<b>0.2386</b>	<b>0.6436</b>	<b>0.4842</b>
<b>10</b>		<b>0.3590</b>	<b>0.2559</b>	<b>0.0571</b>	<b>0.2101</b>
<b>Toe web</b>		<b>1</b>	<b>0.3750</b>	<b>0.2584</b>	<b>0.4344</b>
	<b>2</b>	<b>0.3093</b>	<b>0.2442</b>	<b>0.9739</b>	<b>0.0923</b>
	<b>3</b>	<b>0.2712</b>	<b>0.2411</b>	<b>0.7965</b>	<b>0.4797</b>
	<b>4</b>	<b>0.2182</b>	<b>0.1744</b>	<b>0.6830</b>	<b>0.4445</b>
	<b>5</b>	<b>0.2857</b>	<b>0.1760</b>	<b>0.9958</b>	<b>0.4401</b>
	<b>6</b>	<b>0.4159</b>	<b>0.2263</b>	<b>0.9366</b>	<b>0.1557</b>
	<b>7</b>	<b>0.1818</b>	<b>0.1859</b>	<b>0.0035</b>	<b>0.0720</b>
	<b>8</b>	<b>0.2685</b>	<b>0.2313</b>	<b>0.2925</b>	<b>0.2918</b>
	<b>9</b>	<b>0.2857</b>	<b>0.2464</b>	<b>0.8801</b>	<b>0.4091</b>
	<b>10</b>	<b>0.3373</b>	<b>0.2477</b>	<b>0.5423</b>	<b>0.4714</b>
<b>Inguinal crease</b>	<b>1</b>	<b>0.2500</b>	<b>0.1676</b>	<b>0.9998</b>	<b>0.9192</b>
	<b>2</b>	<b>0.2000</b>	<b>0.1395</b>	<b>0.9981</b>	<b>0.9188</b>
	<b>3</b>	<b>0.2500</b>	<b>0.2694</b>	<b>1.0000</b>	<b>0.9189</b>
	<b>4</b>	<b>0.3333</b>	<b>0.2571</b>	<b>1.0000</b>	<b>0.9189</b>
	<b>5</b>	<b>0.1667</b>	<b>0.1840</b>	<b>0.9999</b>	<b>0.9190</b>
	<b>6</b>	<b>0.3333</b>	<b>0.1949</b>	<b>0.9998</b>	<b>0.9191</b>
	<b>7</b>	<b>0.3276</b>	<b>0.0930</b>	<b>0.9351</b>	<b>0.2739</b>
	<b>8</b>	<b>0.3333</b>	<b>0.2169</b>	<b>1.0000</b>	<b>0.9189</b>
	<b>9</b>	<b>0.2222</b>	<b>0.2558</b>	<b>0.9996</b>	<b>0.9191</b>
	<b>10</b>	<b>0.2857</b>	<b>0.2359</b>	<b>1.0000</b>	<b>0.9190</b>

**Table S7. Intrapersonal vs. Interpersonal variation for four body sites.**

Intrapersonal and interpersonal variations were determined by Jaccard (community membership) and Theta (community structure). Intrapersonal variation is calculated by comparing left and right symmetric sites on the same individual. Interpersonal variation is calculated by comparing an individual to others surveyed at the same body site. Four body sites are shown: plantar heel, toenail, toe web, and inguinal crease. The data represented in this table is displayed graphically in Figure S4.

Body site	HV	Jaccard Intra	Jaccard Inter	Theta Intra	Theta Inter
Antecubital crease	4	0.2074	0.1414	0.9981	0.8764
	6	0.2783	0.1402	0.9616	0.8692
	7	0.277	0.1333	0.7877	0.6234
	8	0.2522	0.1357	0.9797	0.7751
	9	0.1515	0.119	0.9995	0.8752
	10	0.2762	0.1266	0.9992	0.8782
External auditory canal	4	0.1885	0.1814	0.9962	0.9978
	6	0.625	0.3315	1	0.9995
	7	0.2604	0.2907	0.9999	0.9995
	8	0.5833	0.3184	1	0.9995
	9	0.3214	0.2658	1	0.9995
	10	0.2667	0.2902	0.9999	0.9995
Hypothenar palm	4	0.3172	0.1628	0.9182	0.7732
	6	0.2593	0.1750	0.9919	0.8167
	7	0.3396	0.1765	0.8322	0.3941
	8	0.1745	0.1158	0.9900	0.6787
	9	0.1809	0.1218	0.9988	0.8064
	10	0.2475	0.1358	0.9996	0.8041
Inguinal crease	4	0.2667	0.2291	1.0000	0.9185
	6	0.3333	0.1776	0.9998	0.9194
	7	0.3412	0.0675	0.9551	0.5984
	9	0.2361	0.2350	0.9998	0.9186
	10	0.1984	0.1934	1.0000	0.9186
	Nare	4	0.1455	0.1661	0.9998
6		0.2348	0.1893	0.9994	0.8236
7		0.3462	0.1221	0.7747	0.227
8		0.3581	0.1143	0.9412	0.7122
9		0.1538	0.1244	0.9934	0.8073
10		0.75	0.1688	1	0.8028
Plantar heel	4	0.3266	0.2796	0.7366	0.3864
	6	0.3058	0.2634	0.7867	0.2212
	8	0.3414	0.2804	0.8349	0.4043
	9	0.2990	0.2645	0.6590	0.4040
	10	0.3876	0.2832	0.8694	0.4772
	Retroauricular crease	4	0.4167	0.3889	1.0000
6		0.1270	0.2887	1.0000	0.9998
7		0.1833	0.2323	1.0000	0.9998
8		0.3250	0.2144	0.9989	0.9993
9		0.6250	0.3784	1.0000	0.9998
10		0.4167	0.3516	1.0000	0.9998
Toenail	4	0.2156	0.2267	0.6760	0.4236
	6	0.4015	0.2570	0.8011	0.2835
	8	0.2324	0.2227	0.6988	0.4060
Toe web	4	0.1844	0.1897	0.3433	0.2890
	6	0.3824	0.2380	0.5846	0.2845
	7	0.2531	0.2182	0.2582	0.2556
	8	0.3023	0.2383	0.6036	0.3795
	10	0.3262	0.2472	0.6601	0.4422
	Volar forearm	4	0.2844	0.1564	0.9457
6		0.2068	0.1525	0.9860	0.8340
7		0.2837	0.1407	0.7172	0.4404
8		0.1630	0.1242	0.8479	0.7019
9		0.2930	0.1432	0.9995	0.8295
10		0.3415	0.1022	0.9992	0.8246

Body Site	HV	Jaccard Inter	Theta Inter
Back	4	0.2707	0.9998
	6	0.1394	0.9996
	7	0.1200	0.9997
	8	0.3758	0.9998
	9	0.4291	0.9998
	10	0.3610	0.9998
Glabella	4	0.4001	0.9685
	6	0.3619	0.9686
	7	0.066	0.843
	8	0.2524	0.9687
	9	0.3926	0.9686
	10	0.2917	0.9686
Manubrium	4	0.4254	0.8956
	6	0.3437	0.8960
	7	0.0615	0.4785
	8	0.3247	0.8957
	9	0.3857	0.8955
	10	0.4346	0.8954
Occiput	4	0.2553	0.8712
	6	0.3282	0.8603
	7	0.3132	0.8657
	8	0.3122	0.8155
	9	0.4941	0.8738
	10	0.4130	0.5572

**Table S8. Temporal analysis of all body sites in the resampled HVs.**

Longitudinal stability of fungal microbial community membership and structure over time are calculated as Jaccard and Theta, respectively, within mothur. This analysis compares initial and return sampling for six HVs (4,6,7,8,9,10). HV7 was excluded as an outlier from the final analysis. Jaccard and Theta values range from 0 to 1 with larger values representing greater stability. Longitudinal community membership and structure data are displayed graphically in Figure S6.